Closed-form Bias Reduction for Shape Estimation with Polygon Models

Florian Faion, Maxim Dolgov, Antonio Zea, and Uwe D. Hanebeck
Intelligent Sensor-Actuator-Systems Laboratory (ISAS)
Institute for Anthropomatics and Robotics
Karlsruhe Institute of Technology (KIT), Germany
florian.faion@kit.edu, maxim.dolgov@kit.edu, antonio.zea@kit.edu, uwe.hanebeck@ieee.org

***Abstract*—We look at the task of estimating the parameters of a geometric constraint from noisy points in 2D. The classical approach of minimizing the Euclidean distance error between points and constraint generally yields biased estimates for non-linear constraints and higher noise levels. To deal with this issue, the expected distribution of the distance error can be explicitly incorporated in the estimator. However, for piecewise linear constraints, e.g., polygons, only computationally demanding sampling-based approaches are available. We propose two major contributions in order to resolve this issue. First, we derive closed-form expressions for the probability density of the signed distance between noisy points and a polygon angle. Second, based on this result, we develop a bias reduction method for polygons, which can be calculated in closed-form as well. We demonstrate that the quality of our approach can compete with its sampling-based alternatives, but only demands a fraction of their computational cost.**

I. Introduction

Fitting a potentially time-varying geometric constraint to noisy points (with distortion in all dimensions) is a classical problem in many fields related to computer vision, robotics, or economics. The probabilistically correct approach to solving such a so called errors-in-variables problem is explicitly modeling the probability for each point in the constraint, to generate a measurement [1], [2], which is known as Spatial Distribution Model (SDM). However, using SDMs is computationally demanding for more complex constraints, and requires detailed knowledge about the measurement principle. Another straightforward approach is minimizing a distance-related expression between points and curve [3]. Typically, the minimal Euclidean distance is used in this context and related approaches include orthogonal least squares [4], and the iterative closest point algorithm [5].

A. Estimation Bias

However, it is well known that this traditional estimation approach, also referred to as geometric fitting [6], produces biased estimates for all parameters that encode nonlinearity of the constraint, e.g., the radius of a circle [1], the axes of an ellipse [7], or the angle of a polygon corner. This bias originates from an incorrect data association of points to the constraint, which is implicitly performed when calculating the minimal distance [8]. Unfortunately, this Greedy Association Model (GAM) becomes increasingly incorrect with higher nonlinearity and noise [9] and, in turn, results in increasing bias. In consequence, dealing with errors-in-variables problems is a difficult task as Griliches pointed out in [10]: "In short, errors in variables are bad enough in linear models. They are likely to be disastrous to any attempts to estimate additional nonlinearity or curvature parameters."

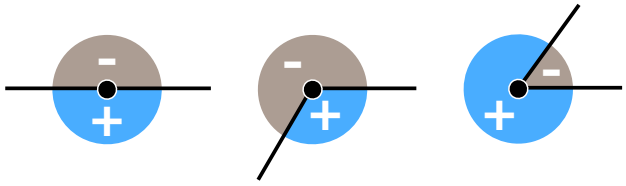

(a) Balanced. (b) Imbalanced. (c) Very imbalanced.

Fig. 1: Bias in the estimated parameters originates from an imbalanced ratio of measurements occurring on both sides of a constraint. In each of the three examples, the gray and blue areas indicate, where measurements will originate from a single source (filled black circle). Naïve distance minimization imposes a perfect balance, which is generally not true (b,c).

Despite of this pessimistic perspective, there are approaches to reduce bias by predicting its effect on the minimal distance from the constraint's nonlinearity and the measurement noise [11], [7], [8]. An example is shown in Fig. 1, where the expected bias in the minimal distance is proportional to the imbalance of probability mass for measurements occurring on both sides of the constraint [8]. In [12], we showed that bias-reduction techniques that compensate for this imbalance are closely related to the statistical concept of partial likelihood [13]. For several special cases, there are even closed-form solutions available, including circles [14], ellipses [6], and more general differentiable curve constraints [7]. However, when it comes to non-differentiable constraints or constraints not differentiable everywhere, such as open and closed polygonal curves, bias reduction has to be performed by constructing complex levelsets [15], or by using numerical approaches such as sampling [8]. This drawback leads us to the contribution presented in this paper.

B. Contribution

We derive a likelihood with closed-form bias reduction that can be used to design an estimator for the parameters of a polygon based on 2D measurements with noise in both dimensions.

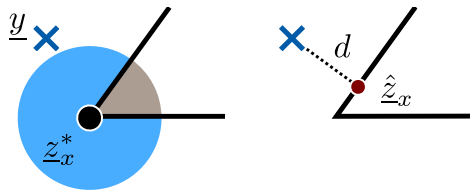

(a) Gaussian noise. (b) Calculating a single distance.

Fig. 2: Visual explanation of the problem statement and the used symbols.

As the essential component, we derive the probability density of the minimal signed Euclidean distance between noisy points and the two legs of an angle, for Gaussian noise with identity covariance matrix, and the source of all points being the intersection of the legs. Based on this theoretical result, we develop a closed-form version of the partial likelihood from [12] for polygonal curves. Our approach marks a significant contribution beyond the state of the art as it (i) extends the class of constraints which can benefit from closed-form bias reduction, and (ii) almost demands no additional computational cost compared to the classical orthogonal least squares approach. In addition, note that essentially any constraint can be approximated as a polygonal curve and, thus, the respective estimator can take advantage of the proposed approach.

II. Formal Problem Statement

Let the desired constraint be represented by a set of parameters, which are aggregated in the state vector $\underline{x}$. This state includes all information to infer the set of all points $\underline{z}_x \in Z_x \subset \mathbb{R}^2$ that satisfy the constraint. For example, parameters of a polygon may include the positions of all its vertices.

The measured points are given as a list of 2D vectors $\underline{y}_1, \ldots, \underline{y}_n$. In order to find an accurate estimate, the relationship between parameters and measurements must be specified. The probabilistic approach to define this relationship is through the likelihood $p(\underline{y}_1, \ldots, \underline{y}_n | \underline{x})$. Assuming the measurement noise to be uncorrelated between all points, the likelihood can be factorized as

$$p(\underline{y}_1, \ldots, \underline{y}_n | \underline{x}) = \prod_{i=1}^{n} p(\underline{y}_i | \underline{x}) \ , \tag{1}$$

which lets us define individual likelihoods $p(\underline{y}_i | \underline{x})$ for each point $\underline{y}_i$. Hence, we can drop the index i for the following considerations. By further assuming the measurement noise to be additive Gaussian with an identity covariance matrix $\mathbf{I}$, the likelihood is given by

$$p(\underline{y} | \underline{x}) = \mathcal{N}(\underline{y}; \underline{z}_x^*, \mathbf{I}) \ , \tag{2}$$

where $\underline{z}_x^*$ denotes the true source of the measurement $\underline{y}$ (see Fig. 2a).

However, due to the measurement noise, we know $\underline{z}_x^*$ only up to the fact that it lies in the constraint $\underline{z}_x^* \in Z_x$. In consequence, in order to be able to evaluate the likelihood, we have to make assumptions about the actually unknown location of the source $\underline{z}_x^*$. Making these assumptions, in turn, is an instance of continuous data association, and in the context of errors in variables, $\underline{z}_x^*$ is referred to as a nuisance parameter [11].

A widely-used heuristic [8] to resolve this association is greedily assuming that a measurement originates from its most likely source in the constraint according to

$$\hat{\underline{z}}_x := \underset{\underline{z}_x \in Z_x}{\arg\max} \ \mathcal{N}(\underline{y}; \underline{z}_x, \mathbf{I}) \ . \tag{3}$$

Then, by substituting the true source $\underline{z}_x^*$ in (2) by its greedy estimate $\hat{\underline{z}}_x$, the likelihood can be evaluated. Note that $\hat{\underline{z}}_x$ is also the source with the minimal Euclidean distance to the measurement $\underline{y}$ for the considered isotropic noise characteristics, as illustrated in Fig. 2b.

Thus, by using this Greedy Association Model (GAM) [8], the estimator will minimize the closest Euclidean distance between measurements and constraint. And, in doing so, GAMs mark the prototype for the popular geometric fitting approach. In order to see this relationship, let us apply the substitution $\underline{e} := \underline{y} - \hat{\underline{z}}_x$ in the likelihood (2), and rearrange it into

$$\begin{aligned} \mathcal{N}(\underline{y}; \hat{\underline{z}}_x, \mathbf{I}) &= c \cdot \exp\left(-\frac{1}{2} \cdot \underline{e}^{\mathrm{T}} \ \mathbf{I} \ \underline{e}\right) \\ &= c \cdot \exp\left(-\frac{1}{2} \|\underline{e}\|^2\right) \\ &\propto \mathcal{N}(\|\underline{e}\|; 0, 1) \ , \end{aligned} \tag{4}$$

where c is a normalization constant and $d^2 := \|\underline{e}\|^2$ is the squared Euclidean distance between measurement and constraint. Using this likelihood in (1), a maximum likelihood estimator would minimize the sum of all squared distances d^2 and, in doing so, would find the least-squares estimate.

At this point, an important observation can be made. The underlying probabilistic model $\mathcal{N}(d; 0, 1)$ actually incorporates the sign (+/-) of the distance d, as the Gaussian distribution has support on the full domain $\mathbb{R}$. More specifically, the sign distinguishes whether a measurement $\underline{y}$ lies on the one or the other side of the constraint, as sketched in Fig. 1. The true constraint in each figure is marked in black, a selected source is drawn as a black dot, and the magnitude of noise around it is schematically indicated by the filled circle. Probability mass for expected measurements from this source on both sides of the constraint is schematically colored in blue and gray.

Based on Fig. 1, we can now conveniently explain the initially mentioned issue that GAM-estimators are generally biased for nonlinear constraints together with noise. The main problem is that, due to the symmetry of $\mathcal{N}(d; 0, 1)$, the GAM imposes that positive and negative distances are perfectly balanced for the true constraint. This assumption indeed holds for the polygon vertex with a *straight* angle in Fig. 1a. However, for any other angle different from π, such as in Fig. 1b and Fig. 1c, the signed distances will always be

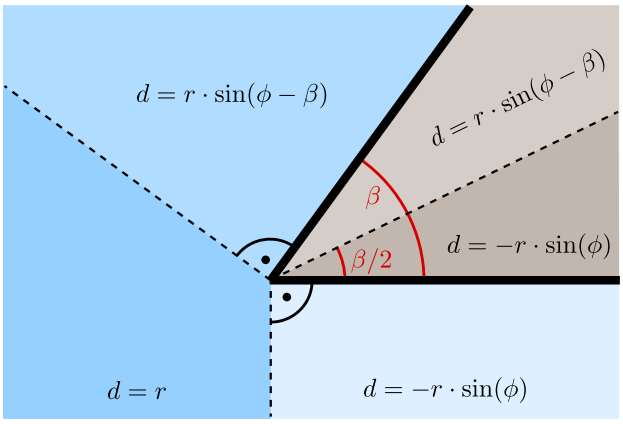

(a) First case: $\beta \in [0; \pi)$.

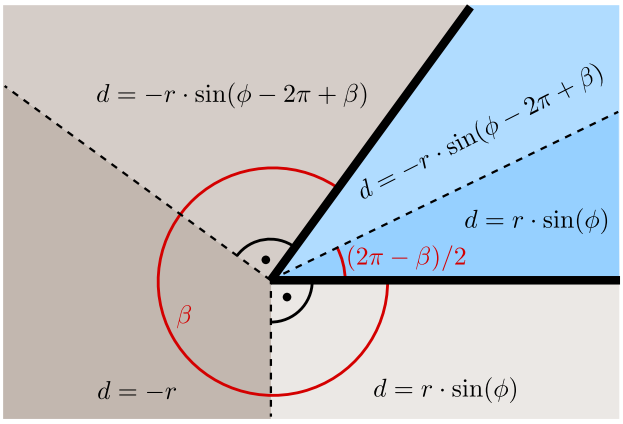

(b) Second case: $\beta \in [\pi; 2\pi)$.

Fig. 3: Partitioning of the integration domain according to the function $a(r, \phi)$. Five different parts can be distinguished for each case. Blue and gray mark parts on one and the other side of the constraint, respectively.

imbalanced. In consequence, by ignoring the specific imbalance, the algorithm will find biased parameters which produce an incorrect constraint with (incorrectly imposed) balanced signed distances.

III. Overview of the Proposed Approach

An effective mechanism to reduce bias in the estimated parameters is replacing the invalid moments $\mu_d = 0$ and $\sigma_d^2 = 1$ by values which are predicted from the current knowledge about nonlinearity and noise [8]. The key idea is to calculate the expected moments of the signed distance at the location $\hat{\underline{z}}_x$ on the curve, and then use them in the likelihood according to

$$p(\underline{y}|\underline{x}) \approx \mathcal{N}\left(d; \mu_d, \sigma_d^2\right) \ . \tag{5}$$

In [12], we showed that $p(\underline{y}|\underline{x})$ can formally be derived from the statistical concept of a partial likelihood, where the measurement $\underline{y}$ is re-parametrized into a component d that encodes "how well" it fits to the constraint, and another component that encodes, "where" on the constraint it corresponds to. Ignoring the unknown "where"-component yields the partial likelihood (5), which we denote as Partial Information Model (PIM).

As the key idea of this paper, we exploit that the density $f_d(d)$ of the minimal signed distances (and its first two moments) between Gaussian samples and a polygon angle can be calculated in closed form, for the case that the measurement source is located on the vertex. In the following, we first derive the closed-form expression for the density $f_d(d)$ and its moments in Sec. IV. Subsequently, in Sec. V, we show how to evaluate the PIM (5) in closed form for polygons as well.

IV. Probability Density of the Signed Distance

In this section, we derive the density (and its first two moments) of the minimal signed distance of samples from a Gaussian to a polygon corner with angle β. We use the convention where $d < 0$ if the sample lies within the angle, and $d > 0$, otherwise. Formally, we derive this density from the probabilistic distance model. For this purpose, let r and ϕ denote the polar coordinates of a sample drawn from $\mathcal{N}(\underline{0}, \mathbf{I})$. In addition, let the considered polygon vertex be located on the origin of the polar coordinate system. Then, the distance d is determined by

$$d = a(r, \phi) \ , \tag{6}$$

where the function $a(\cdot, \cdot)$ computes the minimal signed Euclidean distance of a sample to both legs. In terms of polar coordinates [18], the Gaussian density $\mathcal{N}(\underline{0}, \mathbf{I})$ can be written as

$$f(r, \phi) = \frac{1}{2\pi} \exp\left[-\frac{1}{2} r^2\right] \ . \tag{7}$$

Using (7) and (6), the density of the minimal distance d can be calculated according to

$$f_d(d) = \frac{1}{2\pi} \int_{\Phi} \int_{0}^{\infty} \delta(d - a(r, \phi)) \exp\left[-\frac{1}{2} r^2\right] r \ \mathrm{d}\phi \ \mathrm{d}r \ , \tag{8}$$

where Φ is the angular integration domain, and $\delta(\cdot)$ is the Dirac-δ distribution. In the following, we derive a closed-form solution to this integral with respect to the polygon angle β. In doing so, we distinguish two cases, $0 \leq \beta < \pi$ and $\pi \leq \beta < 2\pi$, both illustrated in Fig. 3.

A. First case: $\beta \in [0; \pi)$

The density of the minimal signed distance of the samples of $\mathcal{N}(\underline{0}, \mathbf{I})$ for $0 \leq \beta < \pi$ is given in the following theorem.

Theorem 1. *For the inner angle β of the body depicted in Fig. 3a with $0 \leq \beta < \pi$, the minimal signed distance probability density $f_d^{(\beta_1)}(d)$ of measurements distributed according to $\mathcal{N}(\underline{0}, \mathbf{I})$ is given by*

$$f_d^{(\beta_1)}(d) = \left(\frac{1}{\sqrt{2\pi}} + \frac{\pi - \beta}{2\pi} d\right) \exp\left[-\frac{1}{2} d^2\right] \Theta(d) + \frac{1}{\sqrt{2\pi}} \exp\left[-\frac{1}{2} d^2\right] \left(1 + \operatorname{erf}\left[\frac{d}{\sqrt{2}} \cot\left(\frac{\beta}{2}\right)\right]\right) \Theta(-d) \ , \tag{9}$$

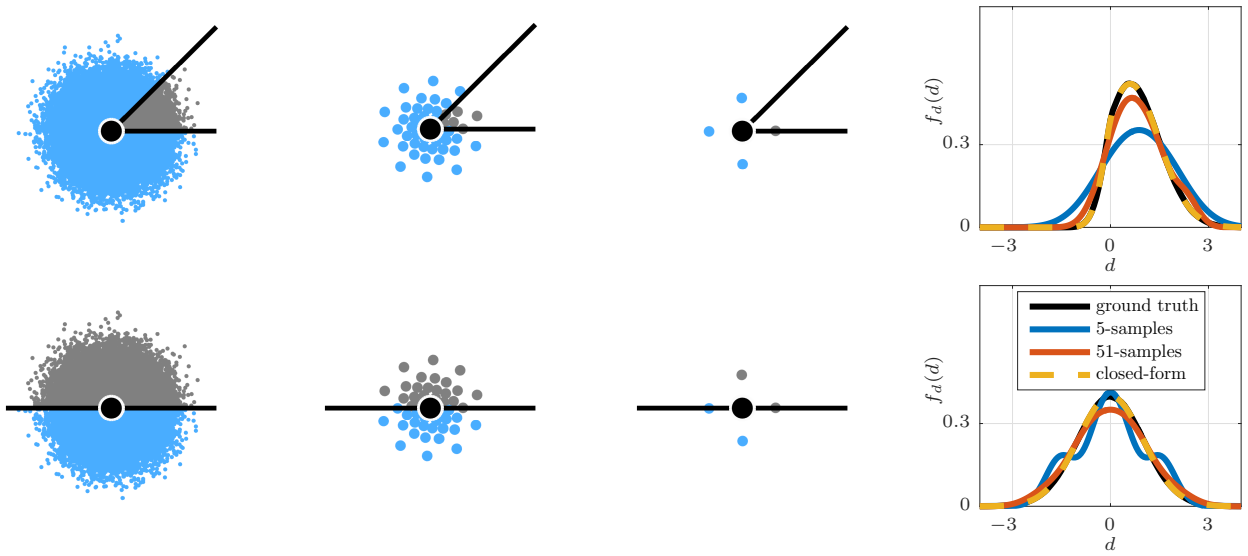

Fig. 4: Calculation of the distribution of the minimal signed distance for two different polygon angles. The respective sampling-based distributions where calculated using a kernel density estimator.

where $\Theta(\cdot)$ *denotes the Heaviside function.*

Proof. The proof is given in Appendix A. □

The mean μ_d and variance σ_d^2 of $f_d(d)$ can be obtained using the results of the following lemma.

Lemma 1. *The first and second moments of the minimal signed distance probability density* $f_d^{(\beta_1)}(d)$ *of measurements distributed according to* $\mathcal{N}(\underline{0}, \mathbf{I})$ *are given by*

$$\mathrm{E}\{d\} = \frac{\pi - \beta + 2\cos(\frac{\beta}{2})}{2\sqrt{2\pi}}$$

and

$$\mathrm{E}\{d^2\} = \frac{3\pi - \beta - \sin(\beta)}{2\pi} \ .$$

Proof. The results of Lemma 1 can be obtained by evaluating the integrals

$$\mathrm{E}\{d\} = \int_{-\infty}^{\infty} d\ f_d^{(\beta_1)}(d)\ \mathrm{d}d \ , \text{ and}$$

$$\mathrm{E}\{d^2\} = \int_{-\infty}^{\infty} d^2 f_d^{(\beta_1)}(d)\ \mathrm{d}d \ .$$

□

B. Second case: $\beta \in [\pi; 2\pi)$

In the following theorem, we give the probability density of the minimal signed distance for measurements being sampled from a standard Gaussian $\mathcal{N}(\underline{0}, \mathbf{I})$.

Theorem 2. *For the inner angle* β *of the body depicted in Fig. 3b with* $\pi \leq \beta < 2\pi$*, the minimal signed distance probability density* $f_d^{(\beta_2)}(d)$ *of measurements distributed according to* $\mathcal{N}(\underline{0}, \mathbf{I})$ *is given by*

$$f_d^{(\beta_2)}(d) = \left(\frac{1}{\sqrt{2\pi}} + \frac{\pi - \beta}{2\pi} d\right) \exp\left[-\frac{1}{2}d^2\right] \Theta(-d) + \frac{1}{\sqrt{2\pi}} \exp\left[-\frac{1}{2}d^2\right] \left(1 + \mathrm{erf}\left[\frac{d}{\sqrt{2}} \cot\left(\frac{\beta}{2}\right)\right]\right) \Theta(d) \ . \tag{10}$$

Proof. Analogously to Theorem 1. □

The results given in the following lemma can be used to calculate the first two moments of $f_d^{(\beta_2)}(d)$.

Lemma 2. *The first and second moments of the minimal signed distance probability density* $f_d^{(\beta_2)}(d)$ *of measurements distributed according to* $\mathcal{N}(\underline{0}, \mathbf{I})$ *are given by*

$$\mathrm{E}\{d\} = \frac{\pi - \beta + 2\cos(\frac{\beta}{2})}{2\sqrt{2\pi}}$$

and

$$\mathrm{E}\{d^2\} = \frac{\pi + \beta + \sin(\beta)}{2\pi} \ .$$

Proof. Analogously to Lemma 1. □

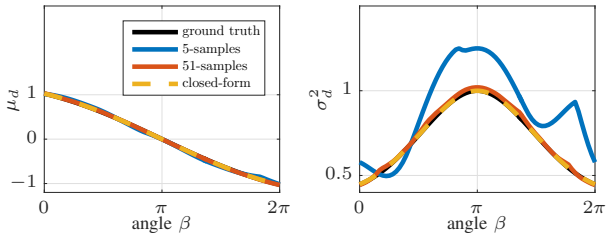

(a) Mean. (b) Variance.

Fig. 5: Approximation quality of the moments of $f_d(d)$.

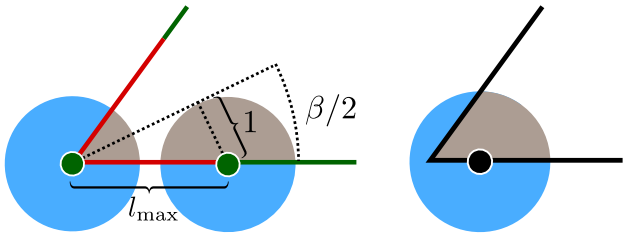

(a) (b)

Fig. 6: Sketch of the applied interpolation.

C. Discussion

By comparing the results from both lemmas, it can be seen that the first moments are equal and the second ones differ. In consequence, we obtain

$$\mu_d := \mathrm{E}\{d\} = \frac{\pi - \beta + 2\cos(\frac{\beta}{2})}{2\sqrt{2\pi}} \tag{11}$$

for the mean and

$$\sigma_d^2 := \mathrm{E}\{d^2\} - \mathrm{E}\{d\}^2 = \begin{cases} \frac{3\pi-\beta-\sin(\beta)}{2\pi} - \mu_d^2 & \text{if } \beta \in [0;\pi) \\ \frac{\pi+\beta+\sin(\beta)}{2\pi} - \mu_d^2 & \text{otherwise} , \end{cases} \tag{12}$$

for the variance of the minimal signed distance. The full densities $f_d^{(\beta_1)}(d)$ and $f_d^{(\beta_2)}(d)$ can be aggregated into $f_d(d)$ analogously using the case function.

Now that we have the desired closed-form expressions, we can compare them to their sampling-based alternatives, available in literature [12]. In Fig. 4, the density $f_d(d)$ is drawn for two example angles. Besides the closed-form approach, we derived kernel densities using 10^7 random samples (for "ground truth") on the one hand, and two sets of deterministically calculated samples on the other hand. For the 51 and 5 deterministic samples (shown in the figure), we used the approaches proposed in [16] and [17], respectively. As can be seen from the figure, the closed-form expression for $f_d(d)$ perfectly coincides with the "ground truth", while the 51-samples and 5-samples kernel densities do not achieve this quality.

Nevertheless, as can be seen from Fig. 5, the approximation quality of mean and variance of $f_d(d)$ is comparable for all approaches and all possible polygon angles $\beta \in [0, 2\pi]$, except for the "5-samples" approach, which yields an incorrect variance. It is interesting to note that for $\beta = \pi$, mean and variance are given by $\mu_d = 0$ and $\sigma_d^2 = 1$, which are the values that are used in the GAM (4). That is why GAMs are unbiased when estimating linear constraints.

V. Closed-form Bias Reduction for Polygons

In this section, we show how to incorporate the closed-form expression for μ_d and σ_d^2 into the PIM-likelihood (5) for polygon constraints. Unfortunately, we cannot always use (11) and (12) directly, as they are only valid for the case that the considered source is located on a vertex. However, generally, we have to deal with situations, where the source is located somewhere else (see Fig. 6b). However, the closed-form solution is valid for (i) the polygon vertices themselves, and (ii) for all sources with a larger distance than a given threshold $l_{\max}$ from a vertex, as we can interpret them as vertices with $\beta = \pi$. In Fig. 6a, the "good" parts of the constraint are drawn in green, and the "bad" parts are drawn in red. From the figure, it can be seen that for all sources being closer to the left vertex than $l_{\max}$, the minimal distance would be calculated using the other leg, which would affect the distribution $f_d(d)$. In the following, we propose an approach to approximate the moments of the signed distance for the red part of the constraint by linear interpolation between the known moments of the polygon vertex and the first source, which is not affected by the other leg.

A. Interpolation

For calculating the interpolation range $l_{\max}$, we assume the magnitude of the measurement noise to be the standard deviation $= 1$ (see Fig. 6a). Based on this assumption, $l_{\max}$ can be calculated according to $l_{\max} = 1/\sin(\beta/2)$, using the triangle from the figure. For the interpolation values, we use μ_d and σ_d^2 from (11) and (12) for the vertex and $\mu_d = 0$ and $\sigma_d^2 = 1$ for the first source whose distance exceeds $l_{\max}$. Then, for any other source with a distance $l \in [0, l_{\max}]$ from the vertex, we can apply a linear interpolation in the form of

$$\mu_d(l) = \begin{cases} -\mu_d \cdot \sin(\frac{\beta}{2}) \cdot l + \mu_d & \text{if } l \le l \le l_{\max} \\ 0 & \text{otherwise} , \end{cases} \tag{13}$$

and

$$\sigma_d^2(l) = \begin{cases} (1-\sigma_d^2) \cdot \sin(\frac{\beta}{2}) \cdot l + \sigma_d^2 & \text{if } l \le l_{\max} \\ 0 & \text{otherwise} . \end{cases} \tag{14}$$

Finally, the proposed Partial Information Model with closed-form bias reduction (PIM-CF) is given by

$$p(\underline{y}|\underline{x}) \approx \mathcal{N}\left(d; \mu_d(l), \sigma_d^2(l)\right) . \tag{15}$$

B. Implementation

Evaluating the likelihood for a given state $\underline{x}$ and measurement $\underline{y}$ then requires the following three steps:

1) Find the closest source $\hat{\underline{z}}_x$ to $\underline{y}$ using (3), and calculate the signed distance $d = \pm\|\underline{y} - \hat{\underline{z}}_x\|$.

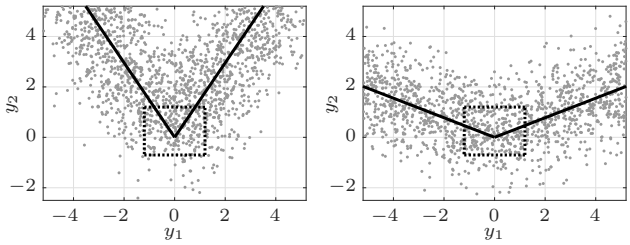

(a) Polygon angle with $\beta = 68°$. (b) Polygon angle with $\beta = 138°$.

Fig. 7: Two instances of the evaluation scenario. For the respective areas within the dashed rectangles, the shape estimates are drawn in Fig. 9.

2) Determine the closest vertex of the polygon to $\hat{\underline{z}}_x$. The angle at this vertex is β and the distance between vertex and $\hat{\underline{z}}_x$ is l.
3) Calculate the moments $\mu_d(l)$ and $\sigma_d^2(l)$ of the signed distance according to (13) and (14).

Finally, with d from step 1, and $\mu_d(l)$, $\sigma_d^2(l)$ from step 3, all components of the likelihood (15) are given, and it can be used in any estimator that employs explicit likelihoods, e.g., a maximum likelihood estimator, particle filter, or the Progressive Gaussian Filter [19], among others. In addition, the proposed approach can be used with estimators which require measurement functions, such as nonlinear Kalman filters, as explained in [12]. For these filters, the measurement equation is given by $0 = h(\underline{x}, \underline{y}, v) = \pm\|\underline{y} - \hat{\underline{z}}_x\| - v$, where v is a Gaussian noise term with $v \sim \mathcal{N}(\mu_d, \sigma_d^2)$.

VI. Evaluation

Earlier in Sec. IV-C, we already validated the correctness of the closed-form expression for the probability density $f_d(d)$ of the signed distance, and its moments μ_d and σ_d^2. Now, we evaluate the proposed PIM-CF likelihood (15) that incorporates the linear interpolation of the closed-form bias reduction.

A. Experiment

We consider a scenario where the parameters of a non-moving polygon angle are to be estimated from sequentially measured noisy points, as sketched in Fig. 7. The state parameters $\underline{x}$ to be estimated consist of the angle β of the polygon angle, as well as the y_2-component of the vertex (y-intercept). In order to allow for a representative assessment of the proposed likelihood, we consider 36 polygon angles with different ground-truth values β in the range between $\frac{1}{4}\pi$ and $\frac{7}{4}\pi$. Two instances of the experiment are shown in Fig. 7a and Fig. 7b, respectively. For each instance of the estimation task, we simulated a total of 2500 point measurements from the polygon angle, where measurement sources were distributed uniformly on the legs within a distance of 10. Then, the measurements were to be processed recursively by the estimators, in 250 packages with 10 points.

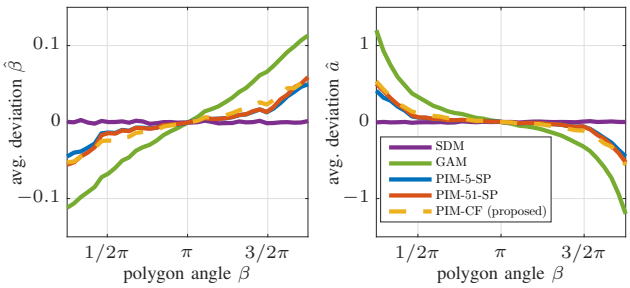

(a) Quality of estimated angles. (b) Quality of estimated y-intercept.

Fig. 8: Mean signed deviation of the estimated parameters from their ground truth-values.

B. Estimators

We implemented likelihoods based on the following models:

- **SDM**: For reference, we consider a Spatial Distribution Model, where we correctly model a uniform distribution for the measurement sources. The involved integral [1] is numerically evaluated, using 100 vertices along the constraint.
- **GAM**: As a representative for the classical orthogonal least squares approach, we set up a Greedy Association Model according to (4).
- **PIM-5-SP / PIM-51-SP**: For the Partial Information Model with sampling-based moment-matching [12], we deterministically calculated 5 and 51 samples according to [17] and [16], respectively.
- **PIM-CF (proposed)**: For the proposed Partial Information Model with closed-form moment-matching and linear interpolation we use the implementation according to Sec. V-B.

For all models, we set up recursive Bayesian estimators [20] based on the Progressive Gaussian Filter [19], which includes an explicit likelihood-based measurement update step. For initialization, we set the state parameters $\underline{x}_0$ to their respective ground truth values and the covariance matrix to $\mathbf{C}_{x_0} = 10^{-1} \cdot \mathbf{I}$. Note that we intentionally chose the ground truth here in order to demonstrate that even perfectly initialized estimates drift away from their perfect values when using an incorrect model. In order to encourage this drifting behavior, we incorporate a random walk model with logarithmically decreasing process noise from a magnitude of 10^{-5} down to 10^{-14}. The following results are obtained from 100 runs for each instance of the experiment, i.e., for each ground truth angle β.

C. Results

In Fig. 8, the estimation accuracy can be quantitatively compared. The horizontal axes denote the ground-truth angle used in the respective experiment, and the vertical axes show the *mean signed deviation* of the estimated parameters from their ground truth values. For unbiased estimators, this deviation should be zero. As can be seen from the figure, the

SDM-approach performs best, as it has additional information about the distribution of the measurement sources. Again, it is important to note that this information is typically not available and the biased GAM-approach would be applied (green).

For the PIM-approaches, there are two important observations we can draw from this accuracy analysis. First, all PIM-versions yield a similar bias reduction of about 50% compared to the traditional GAM approach. This result is remarkable, as the proposed PIM-CF only has a fraction of the computational effort compared to its sampling-based alternatives. The second observation is that the bias reduction mechanism of the PIM cannot compensate for all bias. In particular, increasing nonlinearity of the constraint causes larger bias in the parameters. This behavior can be explained based on the studies in [12], where it was shown that increasing nonlinearity of the constraint increases correlation of the ignored association heuristic.

For a more intuitive understanding of the estimation quality, for two example angles, the estimated shapes are drawn in Fig. 9. In each figure, the estimated shapes of all runs are drawn against the ground truth. As can be seen, the GAM approach cannot manage to find the correct parameters at all for the smaller angle, while the PIM approaches, again, yield far better results.

VII. Conclusion

In this paper, we considered the task of estimating the parameters of polygonal constraints (open or closed) and presented two major contributions:

1) we derived a closed-form expression for the density (and its first two moments) of the minimal signed distance between noisy points and the two legs of an angle, for Gaussian noise, and the source of all points being the intersection of the legs, and
2) based on the closed-form moments, we proposed a Partial Information Model for polygonal constraints that yields a bias-reduced estimator, and where the bias correction can be calculated in closed-form.

In a synthetic benchmark scenario, we showed that the resulting estimator is able to compete with the quality of state-of-the-art bias correction by only requiring a fraction of their computational cost. Subsequent work includes, e.g., improving the interpolation mechanism, or derivation of closed-form expressions for higher-dimensional polyhedrons.

Appendix A
Proof of Theorem 1

For $f_d^{(\beta_1)}(d)$, it holds

$$\begin{aligned} f_d^{(\beta_1)}(d) &= \int_0^{2\pi}\int_0^{\infty} f(d,r,\phi)\ \mathrm{d}r\ \mathrm{d}\phi \\ &= \int_0^{2\pi}\int_0^{\infty} f(d|r,\phi) f(r,\phi)\ \mathrm{d}r\ \mathrm{d}\phi\ , \end{aligned} \tag{16}$$

where $f(r,\phi)$ is the Gaussian probability density function $\mathcal{N}(0,\mathbf{I})$ in polar coordinates according to (7). The density of d conditioned on r and ϕ can be obtained from (6) according to

$$f(d|r,\phi) = \delta(d - a(r,\phi))\ .$$

For $0 \leq \beta < \pi$, the distance function $a(\cdot,\cdot)$ is given by

$$a(r,\phi) = \begin{cases} -r\sin(\phi)\ , & \text{for } \phi \in [-\frac{\pi}{2}; \frac{\beta}{2}) \\ r\sin(\phi-\beta)\ , & \text{for } \phi \in [\frac{\beta}{2}; \beta + \frac{\pi}{2}) \\ r\ , & \text{for } \phi \in [\beta + \frac{\pi}{2}; \frac{3}{2}\pi)\ . \end{cases}$$

Fig. 3a illustrates $a(r,\phi)$ for $0 \leq \beta < \pi$. Please observe that we define the distance to be positive outside the body and negative inside.

In order to evaluate integral (16), we divide it into a sum of integrals w.r.t. ϕ over different intervals. It can be shown that the integral (16) for $\phi \in [-\pi/2; 0)$ is equal to the integral (16) for $\phi \in [\beta; \beta + \pi/2)$, and the integral (16) for $\phi \in [0; \beta/2)$ is equal to the integral (16) for $\phi \in [\beta/2; \beta)$. Integral (16) for $\phi \in [\beta + \pi/2; 3\pi/2)$ can be evaluated as follows

$$\begin{aligned} f_d^{(\beta_1,1)}(d) &= \frac{1}{2\pi}\int_{\beta+\frac{\pi}{2}}^{\frac{3}{2}\pi}\int_0^{\infty} \delta(d-r)\exp\left[-\frac{1}{2}r^2\right] r\ \mathrm{d}r\ \mathrm{d}\phi \\ &= \frac{1}{2\pi}\int_{\beta+\frac{\pi}{2}}^{\frac{3}{2}\pi}\int_{-\infty}^{\infty} \delta(d-r)\exp\left[-\frac{1}{2}r^2\right] r\Theta(r)\ \mathrm{d}r\ \mathrm{d}\phi \\ &= \frac{\pi-\beta}{2\pi} d\exp\left[-\frac{1}{2}d^2\right]\Theta(d)\ . \end{aligned} \tag{17}$$

For the integral (16) for $\phi \in [-\pi/2; 0)$, it holds

$$\begin{aligned} f_d^{(\beta_1,2)}(d) &= \frac{1}{2\pi}\int_{-\frac{\pi}{2}}^{0}\int_0^{\infty} \delta(d+r\sin(\phi))\exp\left[-\frac{1}{2}r^2\right] r\ \mathrm{d}r\ \mathrm{d}\phi \\ &= \frac{1}{2\pi}\int_{-\frac{\pi}{2}}^{0}\int_{-\infty}^{\infty} \delta(d+r\sin(\phi))\exp\left[-\frac{1}{2}r^2\right] r\Theta(r)\ \mathrm{d}r\ \mathrm{d}\phi \\ &= \frac{1}{2\sqrt{2\pi}}\exp\left[-d^2\right]\Theta(d)\ , \end{aligned} \tag{18}$$

where we used the identity

$$\delta(d+r\sin(\phi)) = \frac{\delta\left(r + \frac{d}{\sin(\phi)}\right)}{|\sin(\phi)|}$$

and the fact that $|\sin(\phi)| = -\sin(\phi)$ in the considered integration interval for ϕ.

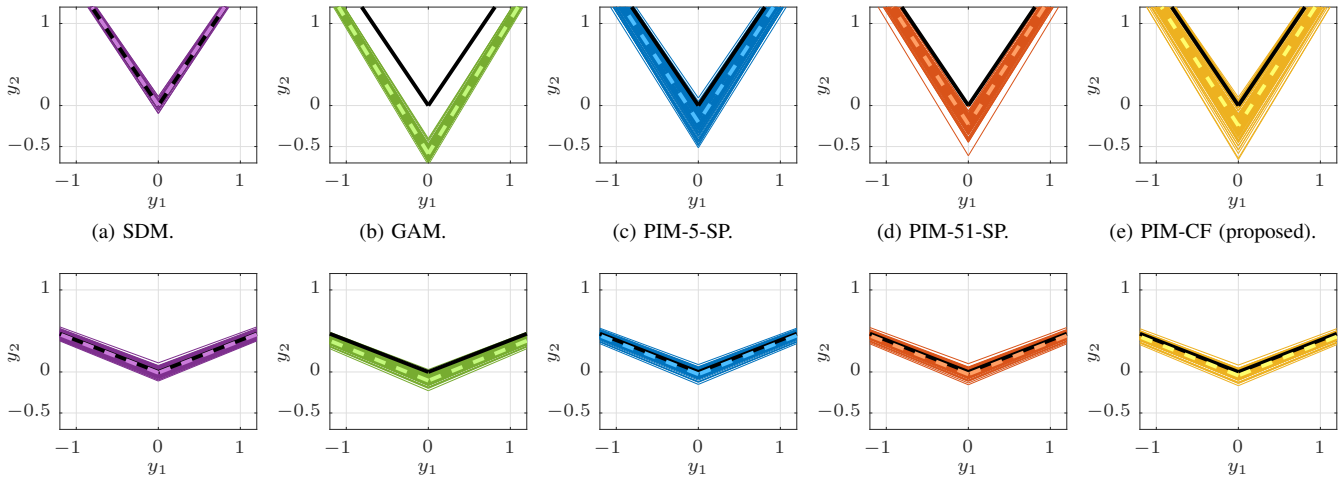

(a) SDM. (b) GAM. (c) PIM-5-SP. (d) PIM-51-SP. (e) PIM-CF (proposed).

(f) SDM. (g) GAM. (h) PIM-5-SP. (i) PIM-51-SP. (j) PIM-CF (proposed).

Fig. 9: Results of the polygon angle experiment for $68°$ (first row) and $138°$ (second row). Estimates of 100 runs are drawn together against the ground truth (black). In addition, the average estimates are drawn as dashed lines. The GAM bias increases with higher nonlinearity. The proposed PIM-approach yields a comparable quality to its sampling-based alternatives.

Finally, the integral (16) for $\phi \in [0; \beta/2)$ is given by

$$
\begin{aligned}
f_d^{(3)}(d) &= \frac{1}{2\pi} \int_0^{\frac{\beta}{2}} \int_0^{\infty} \delta(d + r\sin(\phi)) \exp\left[-\frac{1}{2}r^2\right] r \; \mathrm{d}r \; \mathrm{d}\phi \\
&= \frac{1}{2\pi} \int_0^{\frac{\beta}{2}} \int_{-\infty}^{\infty} \delta(d + r\sin(\phi)) \exp\left[-\frac{1}{2}r^2\right] r\Theta(r) \; \mathrm{d}r \; \mathrm{d}\phi \\
&= \frac{1}{2\sqrt{2\pi}} \exp\left[-\frac{1}{2}d^2\right] \left(1 + \operatorname{erf}\left[\frac{d}{\sqrt{2}} \cot\left(\frac{\beta}{2}\right)\right]\right) \Theta(-d) \; .
\end{aligned} \tag{19}
$$

Combining (17), (18), and (19), we obtain

$$
\begin{aligned}
f_d^{\beta_1}(d) &= f_d^{(\beta_1,1)}(d) + 2f_d^{(\beta_1,2)}(d) + f_d^{(\beta_1,3)}(d) \\
&= \left(\frac{1}{\sqrt{2\pi}} + \frac{\pi - \beta}{2\pi} d\right) \exp\left[-\frac{1}{2}d^2\right] \Theta(d) \\
&+ \frac{1}{\sqrt{2\pi}} \exp\left[-\frac{1}{2}d^2\right] \left(1 + \operatorname{erf}\left[\frac{d}{\sqrt{2}} \cot\left(\frac{\beta}{2}\right)\right]\right) \Theta(-d) \; ,
\end{aligned}
$$

which concludes the proof.

References

[1] M. Werman and D. Keren, "A Bayesian Method for Fitting Parametric and Nonparametric Models to Noisy Data," *IEEE Transactions on Pattern Analysis and Machine Intelligence*, vol. 23, no. 5, pp. 528–534, 2001.

[2] K. Gilholm and D. Salmond, "Spatial Distribution Model for Tracking Extended Objects," *IEE Proceedings - Radar, Sonar and Navigation*, vol. 152, no. 5, p. 364, 2005.

[3] Z. Zhang, "Parameter Estimation Techniques: A Tutorial with Application to Conic Fitting," *Image and Vision Computing*, vol. 15, no. 1, pp. 59–76, 1997.

[4] S. J. Ahn, W. Rauh, and H. J. Warnecke, "Least-squares orthogonal distances fitting of circle, sphere, elipse, hyperbola, and parabola," *Pattern Recognition*, vol. 34, no. 12, pp. 2283–2303, 2001.

[5] P. J. Besl and N. D. McKay, "A Method for Registration of 3-D Shapes," *IEEE Transactions on Pattern Analysis and Machine Intelligence*, vol. 14, no. 2, pp. 239–256, feb 1992.

[6] K. Kanatani and Y. Sugaya, "Unified computation of strict maximum likelihood for geometric fitting," *Journal of Mathematical Imaging and Vision*, vol. 38, no. 1, pp. 1–13, may 2010.

[7] T. Okatani and K. Deguchi, "On Bias Correction for Geometric Parameter Estimation in Computer Vision," in *2009 IEEE Computer Society Conference on Computer Vision and Pattern Recognition Workshops, CVPR Workshops 2009*, 2009, pp. 959–966.

[8] F. Faion, A. Zea, and U. D. Hanebeck, "Reducing Bias in Bayesian Shape Estimation," in *IEEE 17th International Conference on Information Fusion*. Salamanca, Spain: IEEE, 2014, pp. 1–8.

[9] B. Efron, "Bootstrap Confidence Intervals for a Class of Parametric Problems," *Biometrika*, vol. 72, no. 1, pp. 45–58, 1985.

[10] Z. Griliches and V. Ringstad, "Error-in-the-Variables Bias in Nonlinear Contexts," *Econometrica*, vol. 38, no. 2, pp. 368 – 370, 1970.

[11] V. P. Godambe and M. E. Thompson, "Estimating Equations in the Presence of a Nuisance Parameter," *The Annals of Statistics*, vol. 2, no. 3, pp. 568–571, 1974.

[12] F. Faion, A. Zea, M. Baum, and U. D. Hanebeck, "Partial Likelihood for Unbiased Extended Object Tracking," in *Proceedings of the 18th International Conference on Information Fusion*, Washington D. C., USA, 2015, pp. 1022–1029.

[13] W. H. Wong, "Theory of Partial Likelihood," *The Annals of Statistics*, vol. 14, no. 1, pp. 88–123, 1986.

[14] M. Baum, V. Klumpp, and U. D. Hanebeck, "A novel Bayesian method for fitting a circle to noisy points," in *Proceedings of the 13th International Conference on Information Fusion*, Edinburgh, United Kingdom, 2010, pp. 1–6.

[15] A. Zea, F. Faion, and U. D. Hanebeck, "Shape Tracking using Partial Information Models," in *Proceedings of the 2015 IEEE International Conference on Multisensor Fusion and Integration for Intelligent Systems (MFI 2015)*, San Diego, California, USA, sep 2015.

[16] J. Steinbring and U. D. Hanebeck, "LRKF Revisited: The Smart Sampling Kalman Filter (S2KF)," *Journal of Advances in Information Fusion*, vol. 9, no. 2, pp. 106–123, 2014.

[17] S. J. Julier and J. K. Uhlmann, "Unscented filtering and nonlinear estimation," *Proceedings of the IEEE*, vol. 92, no. 3, pp. 401–422, 2004.

[18] A. Papoulis and S. U. Pillai, *Probability, random variables. and stochastic processes*. Tata McGraw-Hill Education, 2002.

[19] J. Steinbring and U. D. Hanebeck, "Progressive Gaussian Filtering Using Explicit Likelihoods," in *Proceedings of the 17th International Conference on Information Fusion*, Salamanca, Spain, 2014.

[20] Z. Chen, "Bayesian Filtering : From Kalman Filters to Particle Filters, and Beyond," *Statistics*, vol. 182, no. 1, pp. 1–69, 2003.